



DeltaE Modelling and Experimental Study of a Standing Wave Thermoacoustic Test Rig

Open
Access

Fatimah Al Zahrah Mohd Saat^{1,2,*}, Dahlia Johari^{1,*}, Ernie Mattokit^{1,2}

¹ Fakulti Kejuruteraan Mekanikal, Universiti Teknikal Malaysia Melaka, Hang Tuah Jaya, 76100 Durian Tunggal, Melaka, Malaysia

² Centre for Advanced Research on Energy, Universiti Teknikal Malaysia Melaka, Hang Tuah Jaya, 76100 Durian Tunggal, Melaka, Malaysia

ARTICLE INFO

ABSTRACT

Article history:

Received 2 May 2019

Received in revised form 12 June 2019

Accepted 3 July 2019

Available online 15 August 2019

Thermoacoustics is a principle of sciences that could be used to create an alternative green and sustainable technology for a cooler or a generator. Unfortunately, the fluid dynamics of the oscillatory flow within thermoacoustic environment is less understood especially as the flow conditions change to higher values of operating conditions. This leads to difficulties in design practices of the system. In this paper, a test of an experimental rig for the investigation of fluid dynamics of an oscillatory flow inside a standing-wave thermoacoustic rig with two different flow frequencies are reported. An experimental setup was build and numerical modelling is also solved using a thermoacoustic software known as DeltaE. The rig consisted of a quarter wavelength resonator attached to a loudspeaker that acts as an acoustic driver. A structure known as 'stack' is located at a location of approximately 0.19λ from the pressure antinode. Experimental results showed that the resonance frequency of the two setups are 14.2 Hz and 23.6 Hz, respectively. Measured velocity and pressure at several locations are analysed and the results indicated that the thermoacoustic flow conditions are achieved. The rig could be used for further and deeper investigations of fluid dynamics behaviour for oscillatory flow of thermoacoustics.

Keywords:

Thermoacoustics; DeltaE; thermal-fluids;
oscillatory flow

Copyright © 2019 PENERBIT AKADEMIA BARU - All rights reserved

1. Introduction

Nowadays, cooler and power source are to be considered as basic human needs. Power source is needed to supply electricity to almost all devices such as a bulb, a refrigerator, an air-conditioner, a television, a radio and it is even needed to run security system for most countries [1, 2]. The usage of power is increasing exponentially with years due to the increase of population and needs [2, 3]. Researches in the area of heat transfer enhancements, for an example, are currently being investigated by many with an aim to improve the energy transfer in most energy systems [4]. Nevertheless, the growth of technology has also escalated the concerns about the impact of the

* Corresponding author.

E-mail address: fatimah@utem.edu.my (Fatimah Al Zahrah Mohd Saat)

* Corresponding author.

E-mail address: dahliajohari93@gmail.com (Dahlia Johari)

technology on the environment. Concerns are rising as the natural resources are now depleting and the 'global warming' effect as well as pollution issues are increasing. There is an urgent need for a green and sustainable technology that could provide human needs but at the same time cause no harm to environment. Thermoacoustics is a principle of science that can offer such requirements [5, 6, 9]. Thermoacoustics can be used to produce a generator/electric power or a cooler/heater if specific conditions are met [6-12].

The acoustical to thermal conversions of energy relies heavily on the fluid dynamics behaviour of an oscillatory flow of the fluids inside the system. At this moment, the fluid dynamics of flow inside the system is not well known. Hence, investigation is needed in this direction. Earlier investigations reported many special characteristics such as early stage turbulence, entrance region and non-linear flow related to heat transfer characteristics [13-17]. These investigations are, however, limited to only several specific flow conditions. Fluid dynamics change with operating conditions. Hence more investigations are needed to cover the wide range of thermoacoustic flow conditions. For complex flow conditions, such as those found in thermoacoustics, theoretical solutions are only available for linear model [5]. In most real and complex cases, experimental investigations are needed to help understand the complex nature of the fluid dynamics inside thermoacoustic environment. In order to conduct the fluid dynamic study, an experimental rig that is able of producing the correct oscillatory flow of thermoacoustics environment must be build. The system needs to be designed carefully at early stage of investigation to avoid too much expensive expenditure that could end up with wrong setup. In thermoacoustic community, this is usually done through a thermoacoustic software known as DeltaE [5, 18]. The software helps designer to assemble parts of the system into the model and then solve the model so that flow distribution inside the system is in accordance to the thermoacoustic principle. This paper reports the results of modelling works related to a standing wave thermoacoustic system with a quarter wavelength resonator using DeltaE for the purpose of the investigation of fluid dynamics of flow inside a standing wave thermoacoustic environment. New investigation of the effect of flow frequency is reported. Experimental rig that allows investigation of fluid dynamics for two different flow frequencies is described. Results are to be discussed with comparison between theory, experiment and modelling. The proposed rig can be used for fundamental investigations of fluid dynamics of an oscillatory flow inside thermoacoustic environment.

2. Methodology

2.1 DeltaE Modelling

The standing wave thermoacoustic model is solved using a software known as DeltaE. This software solves one-dimensional linear model of thermoacoustics and a shooting-method was used at the boundaries of each segments until convergence is achieved. The linear thermoacoustic models are based on the application of oscillatory flow conditions into the continuity equation, momentum equation and the energy equation [5, 18]. Figure 1 shows the segments that were defined in DeltaE. It consists of a 'Begin' segment that will allow the setting up of the initial values and operating conditions for the numerical modelling. The 'begin' segment is then connected to a 'duct', labelled as '1' in Figure 1 and 2, which represents a loudspeaker.

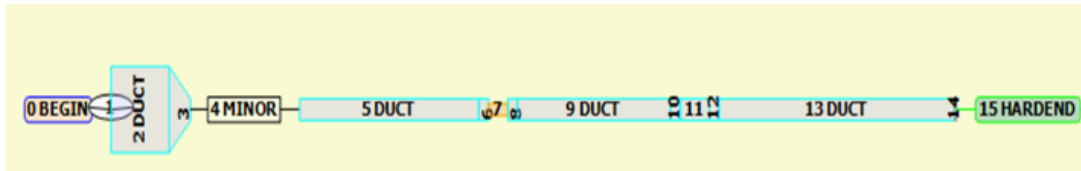


Fig. 1. The 14.2 Hz thermoacoustic model in DeltaE

The loudspeaker is connected to segment '2' that is named as a 'short duct'. This segment is to be considered the box for the loudspeaker and it helps contained the sound that comes out of the loudspeaker. The sound is then channelled into the resonator through segment '3' (a conical duct). Segment '4', which is known as 'minor', is introduced into the model to represent losses of the flow when it is being forced into the resonator through the converging channel. The resonator starts at segment '5' and ends at segment '15'. The total length of the resonator as shown in Figure 1 is 6.6 m. A structure known as 'stack' is located in segment '7' of Figure 1 and it is sandwiched between segments '6' and '8'. The 'stack' is a parallel-plates structure commonly used in thermoacoustics to provide medium for energy exchange between the acoustic wave and the solid surface. This is the place where most thermoacoustic effects take place [5]. The presence of big number of segments in the resonator is due to the design requirement so that the rig can be used for two different flow frequencies. The schematic diagram shown in Figure 1 represents the 14.2 Hz resonator. Investigation is also done for another flow frequency of 23.6 Hz. The DeltaE model for 23.6 Hz is as shown in Figure 2.

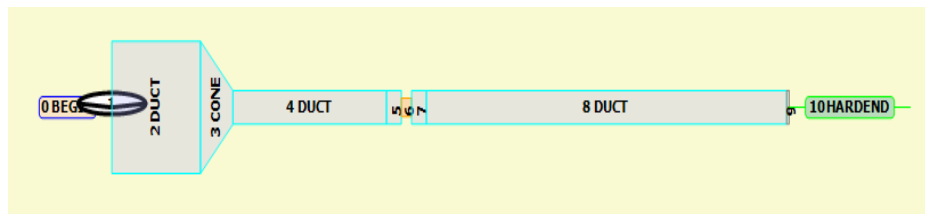


Fig. 2. The 23.6 Hz thermoacoustic model in DeltaE

For high frequency of 23.6 Hz, the total length of the resonator is 3.8 m. Therefore, the total number of segments are now reduced to 10. In this 23.6 Hz model, the stack is located in segment '6' of Figure 2. The models are solved for several cases as summarized in Table 1. The wavelength for air is calculated as $\lambda = c/f$ (where c and f are the speed of sound and the flow frequency, respectively). For the purpose of modelling investigation, the stack is located at two different locations of 0.19λ and 0.11λ relative to the hard end of the resonator (pressure antinode location).

Table 1
 Summary of cases for thermoacoustic models

Case	Frequency (Hz)	Stack's length (mm)	Stack's location
1	14.2	200	0.19λ
2	14.2	200	0.11λ
3	14.2	70	0.19λ
4	23.6	200	0.19λ
5	23.6	70	0.19λ

2.2 Experimental Setup

The experimental rig is as shown in Figure 3. The rig is designed with several segments to allow

for investigations of two flow frequencies. The first rig (as is shown on top of Figure 3) is 6.6 m long while the second rig (the middle diagram) is 3.8 m long. One side of the resonator is connected to a 700 W subwoofer (Model PD180). The input of the loudspeaker is controlled by a function generator and a power amplifier (FLP-MT1201). The loudspeaker is 18 inch in diameter while the resonator is an aluminium duct with a square cross-section of 152.4 mm x 152.4 mm. A loudspeaker box with converging channel is specially designed to connect the subwoofer to the resonator so that standing-wave could be created inside the resonator.

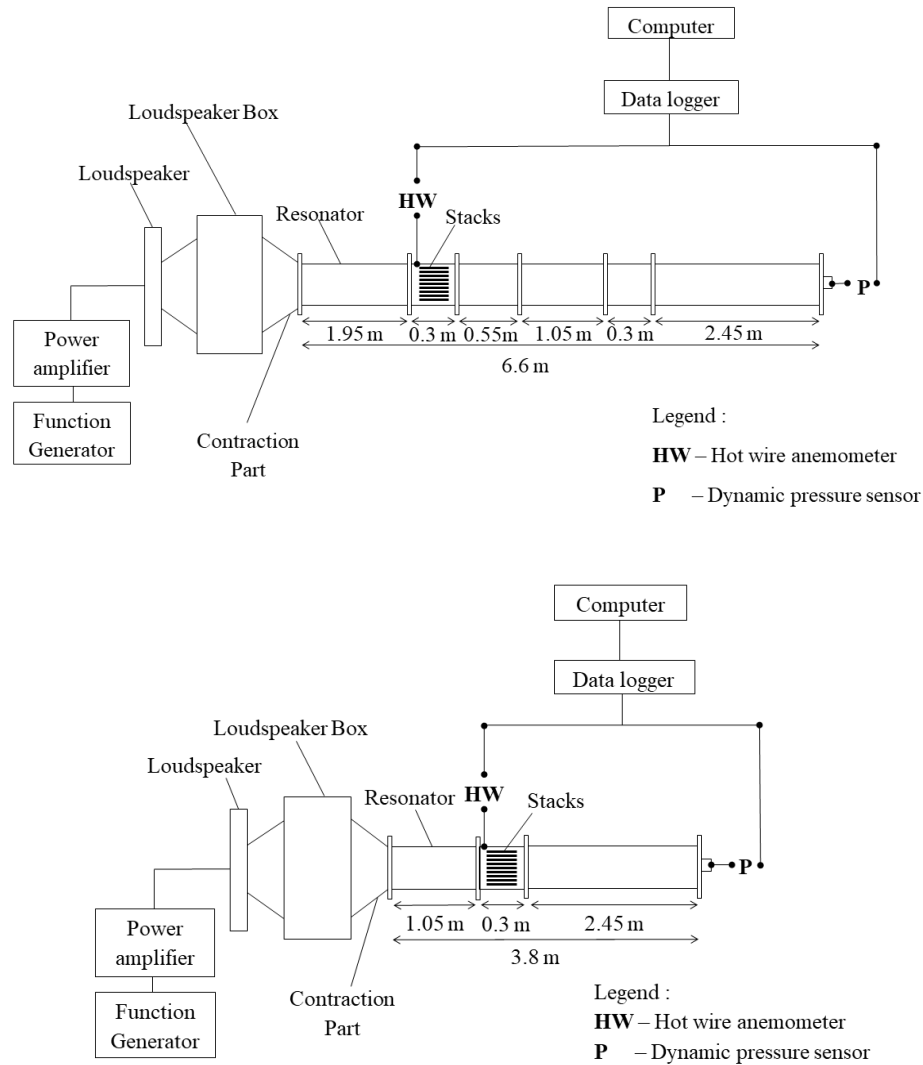


Fig. 3. The sechematic diagram of the 6.6 m rig (top), the 3.8 m rig (middle) and pictures of the real rig (bottom)

For experimental works, the parallel-plate structure known as a ‘stack’ is placed at a location of 0.19λ from the hard-end of the resonator (the pressure antinode). A piezoresistive sensor (Meggit model 8510B) is used for measuring pressure amplitude of the flow and a hot wire (Sentry model ST732) is used to measure velocity. Sensors are connected to a data logger (Dataq DI-718B) that is fitted with signal conditioner (Model DI-8B41-01). Measured data are processed using Windaq software. The resonator is filled with air at atmospheric pressure. It is noteworthy that the two different lengths of resonator lead to different resonance frequencies. In the experimental works, the length of the resonator is achieved by assembling appropriate parts/segments in a similar way as reported for DeltaE models. Dimensions of each parts/segments are given in Figure 3.

3. Results and Discussions

3.1 DeltaE Results

Figure 4 shows the pressure distribution data for cases 1, 2 and 3 as defined earlier in Table 1. The pressure distribution inside an empty resonator (without stack) is shown to be increasing with locations away from the loudspeaker according to the standing wave characteristics. The presence of 200 mm stack in the resonator cause a pressure drop depending on the location of the stack. When the stack is located at 0.19λ , the pressure drop is seen as early as segment 6. For location of 0.11λ , the pressure starts dropping in segment 10. This is as expected following common senses. It is also observed that the pressure values at the locations after the ‘stack’ for cases where ‘stacks’ are placed inside the resonator are bigger compared to the case with an empty resonator. This indicates that the presence of a stack of parallel plates changes the pressure values inside the resonator especially at locations towards the hard end of the resonator.

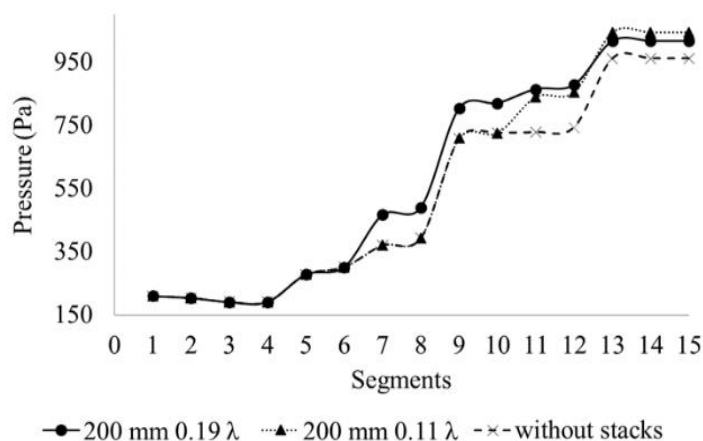


Fig. 4. Pressure distribution for cases 1, 2 and 3 as predicted by DeltaE models

The DeltaE model is then solved for different length of stacks (70 mm vs 200 mm) and the results are as shown in Figure 5. As expected, the pressure drop is smaller for case with stack of shorter length. The presence of the 70 mm long stack has very little impact on pressure distribution inside the resonator.

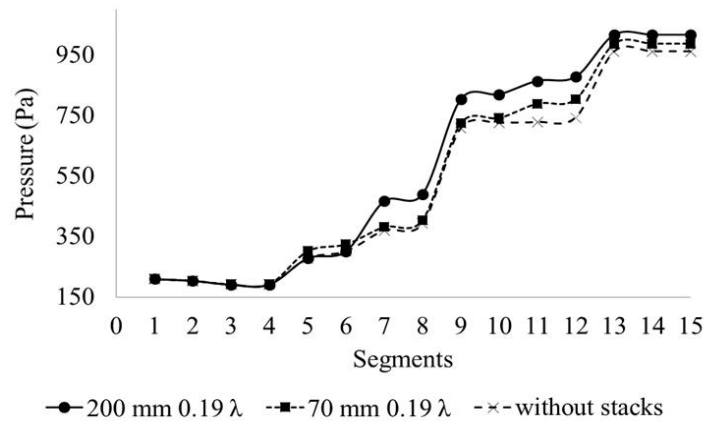


Fig. 5. Pressure distribution for cases 3 and 4 as predicted by DeltaE models

Figure 6 shows comparison of pressure distribution data for two different flow frequencies. In general, pressure distribution inside the resonator at high flow frequency is higher compared to that of the low flow frequency. This is probably due to the different values of drive ratio. High amplitude of pressure may contribute towards higher energy production (based on the understanding that work production is related to the product of pressure and the change of volume). However, high pressure could also lead to losses based on pressure drop value. The balance between the gain and lost should always be considered.

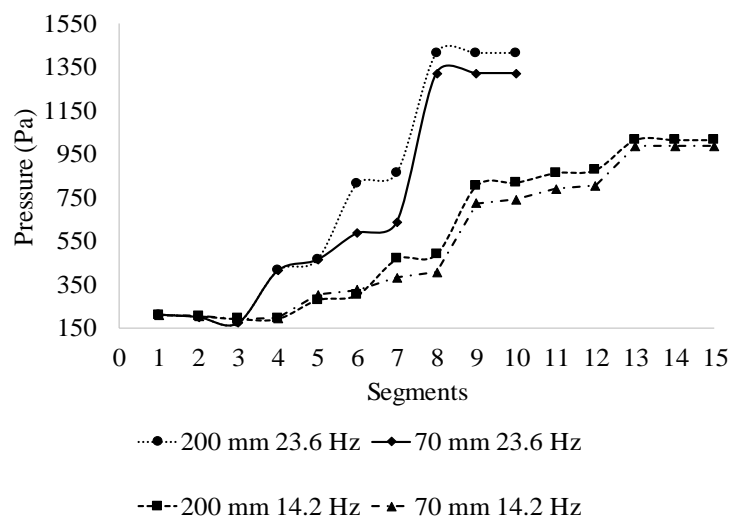


Fig. 6. Pressure distribution for cases with different stack's length and different frequency

As a rule of thumb, length of stack is normally chosen by considering the size of gas displacement. For flow amplitude with drive ratio of up to 2 %, the gas displacement for the cases of 14.2 Hz and 23.6 Hz are estimated at approximately 56 mm and 34 mm, respectively. The working medium flows in oscillatory manner into and out of the stacks' channel on both sides of the ends. Hence, a stack with a minimum length of 112 mm is preferable, otherwise mix of temperature could happen between the two ends of the stack. Ideally, one end is supposed to be hot and the other end should be cold. If mix of temperature happens, thermoacoustic effect will be tampered and system's performance could be affected in a bad way. Although the current study focuses only on the fluid

dynamics aspects, but the practical aspects of the thermoacoustic system should not be put aside. For ease of comparison between cases, the investigation is therefore continued with stack of 200 mm long.

3.2 Experimental Results

3.2.1 Resonance frequency

The experimental rig was designed according to a quarter wavelength criterion. At the early stage of the research works, the experimental design was made based on theoretical calculations. According to calculation, the 6.6 m long resonator is corresponding to a resonance frequency of 13.1 Hz while the 3.8 m long resonator is corresponding to a resonance frequency of 23.1 Hz. However, experiments are needed to confirm the real value of the resonance frequency for the rig because the presence of additional fixtures like the loudspeaker box and segmentations of resonator may lead to changes to the resonance frequency.

Figure 7 shows the experimentally measured resonance frequency of the 6.6 m long and 3.8 m long resonators. The resonance frequency is tested by keeping the voltage input of the loudspeaker at a constant minimum value. The frequency is then varied with an increment of 1 Hz until maximum value of pressure is recorded by the pressure sensor. Figure 7 shows the measured resonance frequency for the 6.6 m long and 3.8 m long resonator, respectively. The drive ratio represents the ratio between the measured value of pressure at antinode and the mean pressure. Results show that the resonance frequency of the 6.6 m long rig is 14.2 Hz and the resonance frequency of the 3.8 m long rig is 23.6 Hz.

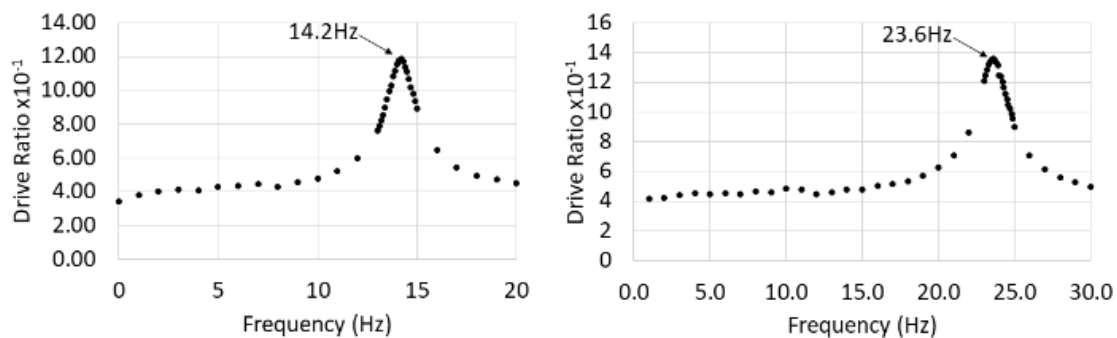


Fig. 7. Resonance frequency for the 6.6 m long resonator (left) and the 3.8 m long resonator (right)

3.2.2 Pressure and velocity distribution along resonator

Measurements are done for pressure and velocity values at several locations along the resonator. The locations are as defined in Figure 8. Locations A to D represent data from a 6.6 m long resonator while locations E and F represent data from a 3.8 m long resonator.

The measured values are also compared to the values predicted by the one-dimensional non-linear thermoacoustic theory. The theoretical results of first order harmonic of velocity amplitude, u_1 , and pressure amplitude, p_1 , are calculated using Eq. (1) and Eq. (2).

$$u_1 = \frac{k \cdot p_a \sin(kx)}{\omega \rho_m} \quad (1)$$

$$p_1 = p_a \cos(kx) \tag{2}$$

The terms k , p_a , x , ω and ρ_m represent the wave number, pressure amplitude at antinode (hard end), location from the antinode, angular velocity and mean density, respectively. The pressure amplitude at location of antinode, p_a , is measured using a piezoresistive sensor that is flushed mounted at the hard end of the resonator. The first order amplitude of pressure, p_1 , and velocity, u_1 , at locations A to F are recorded by placing the piezoresistive sensor and hotwire at that locations. The results are as shown in Figure 9 and 10.

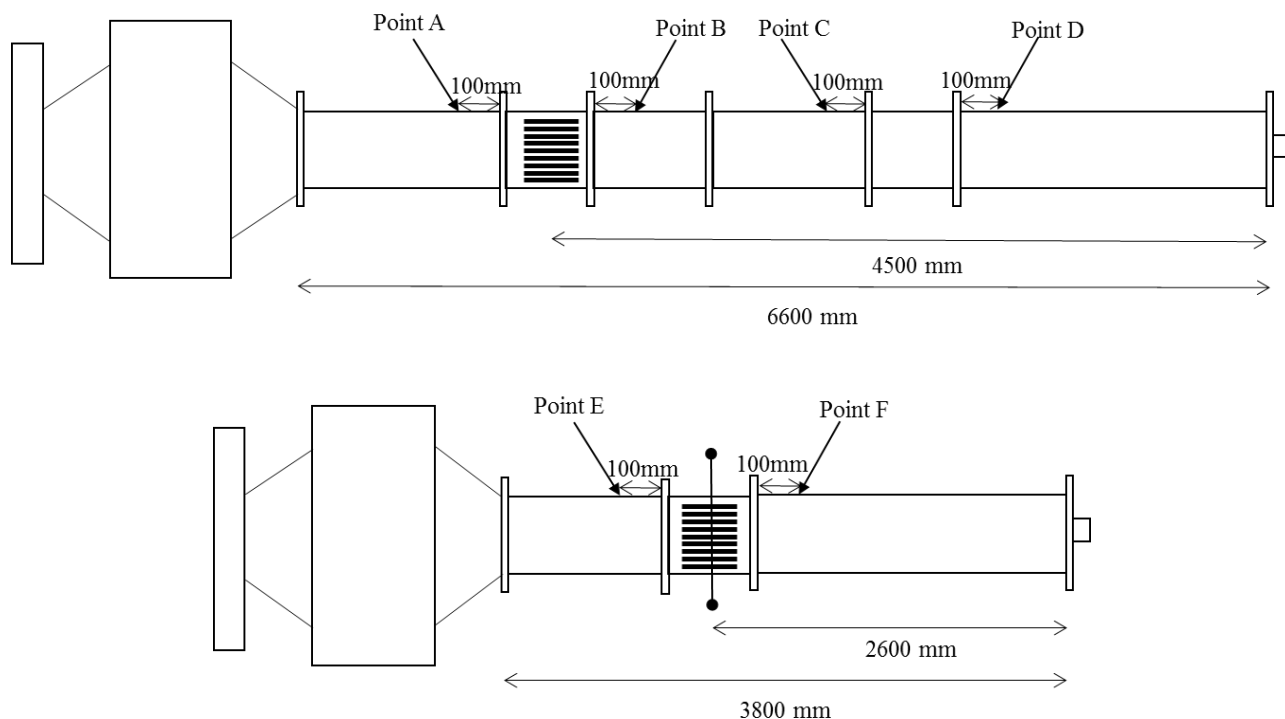


Fig. 8. Locations for measurement points along the resonator of 6.6 m long (top) and 3.8 m long (bottom)

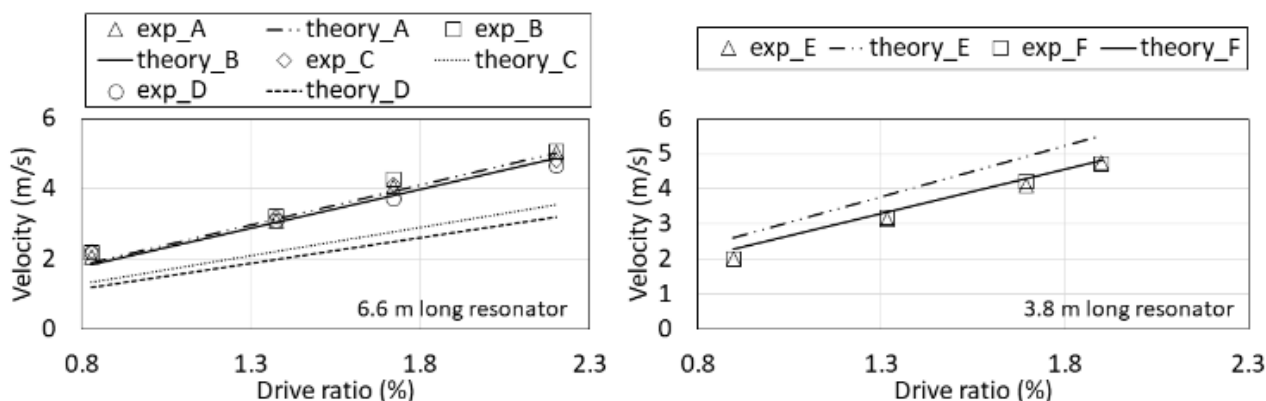


Fig. 9. Comparison between measurement and theoretical values of velocity amplitude along the resonator

There are two aspects that can be looked at. First is the impact of flow amplitude (i.e. drive ratio) and second is the measured locations (locations A to F). In general, Figure 9 shows that both theoretical and experimental values exhibit the same pattern of flow increment as drive ratio

increases.

The same pattern of increment is also observed for pressure values as shown in Figure 10. However, it is interesting to note that the increment of pressure amplitude with drive ratio for the short resonator (i.e. flow frequency of 23.6 Hz) is represented by a pattern that resembles exponential behaviour of change. This is not seen for a low drive ratio of 14.2 Hz (i.e. the 6.6 m long resonator). At low flow frequency, the pressure amplitude increase almost linearly with the increase of drive ratio. Location wise, Figure 9 shows that the velocity amplitude reduces as the flow is approaching the hard end (in the direction from A to D for the 6.6 m long resonator and from E to F for the 3.8 m long resonator). However, the pressure amplitudes increase as the location changes from A to D.

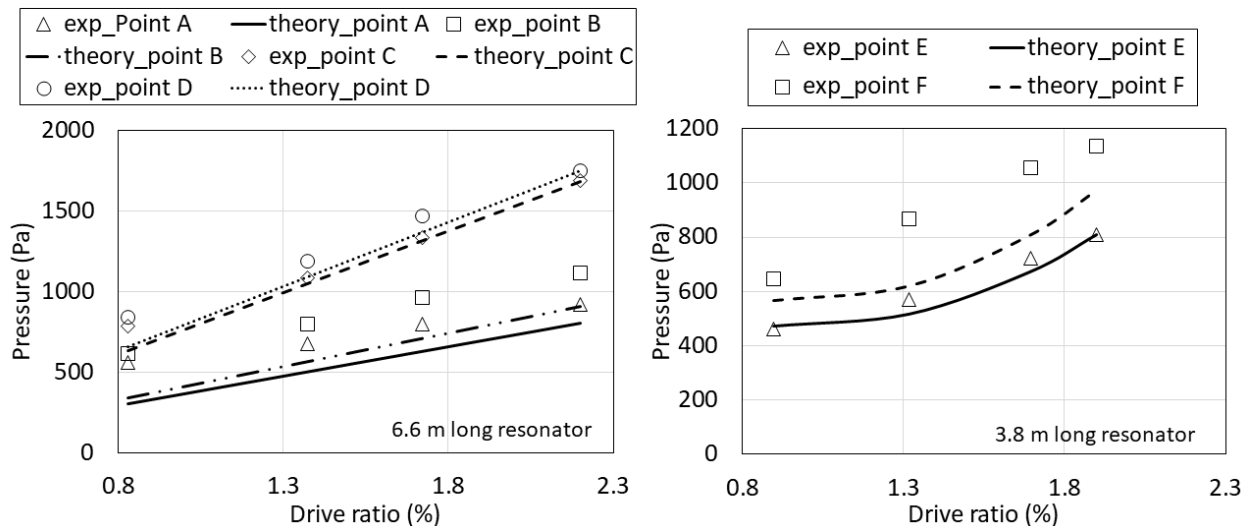


Fig. 10. Comparison between measurement and theoretical values of pressure amplitude along the resonator

The same pattern of velocity reduction and pressure increment with locations are shown by theoretical calculation and the experimentally measured values. In the experiment for the 6.6 m long resonator (i.e. 14.2 Hz), the decrease of velocity from locations A to D are recorded with maximum drop of 0.41 m/s while the theory predicts a reduction of 1.85 m/s. This corresponds to a difference of around 70% which may be related to ‘streaming’ or ‘non-linear’ effects that are not counted in the theoretical equations. Observation of non-linear effects have been reported by many in the past (c.f. [6, 13, 15, 16, 17]). The same observation is also seen for values of pressure, as shown in Figure 10, but the difference in magnitude between experiment and theory is lower (with biggest error of 14%). Nevertheless, the similar pattern of velocity and pressure changes between experiment and theory indicates that a correct thermoacoustic environment have been achieved. Detail investigations will be needed to help understand the difference in magnitude/scale which is expected to be related to the presence of non-linearity of flow in the real condition of the experimental tests.

4. Conclusions

One dimensional nonlinear models of thermoacoustics were solved for two flow frequencies with two different length of stack located at two different locations. The models converged and this indicates that thermoacoustic environment was achieved using the segmented design of the resonator. An experimental setup for a standing wave thermoacoustic rig with a quarter wavelength resonator was also successfully build. The rig was designed with segments that will allow investigation of fluid dynamics study for two different flow frequencies. Experimental measurements showed that

the resonance frequency of the two different setups are 14.2 Hz and 23.6 Hz, respectively. This allow for the new investigation of the effect of flow frequency on fluid dynamics of oscillatory flow inside the system. The rig is now ready to be used for future investigations of the less understood fluid dynamics phenomena of thermoacoustic flow conditions. The investigations that are currently being pursued at Universiti Teknikal Malaysia Melaka involved experimental measurements of fluid flow, flow visualization using Particle Image Velocimetry (PIV) and the use of Computational Fluid Dynamics software so that better insights into fluid dynamics of oscillatory flow across structures inside thermoacoustic system could be gained. The use of vibration suppressor/silencer such as fibers [19] could also be considered in future studies of thermoacoustics for the purpose of reducing vibration that could lead to reduction of unwanted streaming in the thermoacoustic flow environment.

Acknowledgements

The first author would like to thank Prof. Artur J. Jaworski for his valuable input regarding the experimental measurement practices. The research work was funded by Ministry of Education of Malaysia (FRGS/1/2015/TK03/FKM/03/F00274) and was carried out using facilities at the Universiti Teknikal Malaysia Melaka.

References

- [1] Khattak M. A., Tuan Yahya T. M. H., Mohd Sallehudin M. W., Mohd Ghazali M. I., Abdullah N. A., Nordin N. A., Mohd Mohsein Dzakurnain N. A. "Energy Security Policy Shift of North America and Ontario, Canada Following 2003 Power Blackout: A Review." *Progress in Energy and Environment* 4, no. 1 (2018): 14-24.
- [2] Khattak M. A., Yahya T. M. H. T., Sallehudin M. W. M., Ghazali M. I. M., Abdullah N. A. "Global Energy Security and Eastern Europe: A Review." *Journal of Advanced Research Design* 45, no. 1 (2018): 19-42.
- [3] Saidur, R. "Energy consumption, energy savings, and emission analysis in Malaysian office buildings." *Energy policy* 37, no. 10 (2009): 4104-4113.
- [4] Sidik N. A. C., Alawi O. A. "Computational Investigations on Heat Transfer Enhancements Using Nanorefrigerants." *Journal of Advanced Research Design* 1, no. 1 (2014): 35-41
- [5] Swift, Greg W. "Thermoacoustics: A unifying perspective for some engines and refrigerators." *The Journal of the Acoustical Society of America* 113, no.5 (2003): 2379-2381.
- [6] Abdoulla-Latiwish, Kalid OA, Xiaolan Mao, and Artur J. Jaworski. "Thermoacoustic micro-electricity generator for rural dwellings in developing countries driven by waste heat from cooking activities." *Energy* 134 (2017): 1107-1120.
- [7] Agarwal, Harshal, Vishnu R. Unni, K. T. Akhil, N. T. Ravi, S. Md Iqbal, R. I. Sujith, and Bala Pesala. "Compact standing wave thermoacoustic generator for power conversion applications." *Applied Acoustics* 110 (2016): 110-118.
- [8] Bi, Tianjiao, Zhanghua Wu, Limin Zhang, Guoyao Yu, Ercang Luo, and Wei Dai. "Development of a 5 kW traveling-wave thermoacoustic electric generator." *Applied energy* 185 (2017): 1355-1361.
- [9] Saechan, Patcharin, and Artur J. Jaworski. "Thermoacoustic cooler to meet medical storage needs of rural communities in developing countries." *Thermal Science and Engineering Progress* 7 (2018): 164-175.
- [10] Saechan, Patcharin, and Artur J. Jaworski. "Thermoacoustic cooler to meet medical storage needs of rural communities in developing countries—High pressure system." *Thermal Science and Engineering Progress* 8 (2018): 31-46.
- [11] Perier-Muzet, Maxime, Jean-Pierre Bédécarrats, Pascal Stouffs, and Jean Castaing-Lasvignottes. "Design and dynamic behaviour of a cold storage system combined with a solar powered thermoacoustic refrigerator." *Applied Thermal Engineering* 68, no. 1-2 (2014): 115-124.
- [12] Sharify, Esmatullah Maiwand, and Shinya Hasegawa. "Traveling-wave thermoacoustic refrigerator driven by a multistage traveling-wave thermoacoustic engine." *Applied Thermal Engineering* 113 (2017): 791-795.
- [13] Mohd Saat, Fatimah, and Artur Jaworski. "Numerical predictions of early stage turbulence in oscillatory flow across parallel-plate heat exchangers of a thermoacoustic system." *Applied Sciences* 7, no. 7 (2017): 673.
- [14] Jaworski, Artur J., Xiaolan Mao, Xuerui Mao, and Zhibin Yu. "Entrance effects in the channels of the parallel plate stack in oscillatory flow conditions." *Experimental Thermal and Fluid Science* 33, no. 3 (2009): 495-502.
- [15] Mustafa S. H. A, Mohd Saat F. A. Z., Mattokit E. "Numerical study of entrance effects in an oscillatory flow of a standing-wave thermoacoustics." *Journal of Advanced Research in Fluid Mechanics and Thermal Sciences* 43, no. 1 (2018): 149-157.

-
- [16] Kuzuu, Kazuto, and Shinya Hasegawa. "Numerical investigation of heated gas flow in a thermoacoustic device." *Applied Thermal Engineering* 110 (2017): 1283-1293.
- [17] Kuzuu, Kazuto, and Shinya Hasegawa. "Effect of non-linear flow behavior on heat transfer in a thermoacoustic engine core." *International Journal of Heat and Mass Transfer* 108 (2017): 1591-1601.
- [18] Johari D, Mattokit E., Mohd Saat F. A. Z. "Parametric Study of Thermoacoustic System using DeltaE." *Journal of Advanced Research in Fluid Mechanics and Thermal Sciences* 46, no. 1 (2018): 161-168.
- [19] Ismail A. Y., Chen M. F., Azizi M. F., Sis M. A. "Experimental Investigation on the use of Natural Waste Fibres as Acoustic Material of Noise Silencer." *Journal of Advanced Research in Materials Science* 22, no. 1 (2016): 1-10.